1 Pull-Out

Outline: In this chapter we introduce elementary test setups for the pullout of a bar from a cementitious matrix. The goal is set up the playground for questions of test design. Tests are mostly focusing on isolated effects of material behavior, like debonding between two material components. However, it is seldom possible to completely avoid additional effects. The pull-out test setup can be conveniently used to demonstrate the dilemmas involved in a test setup design. By raising these questions we shall motivate the deeper look at the material behavior versus the structural behavior in Chapter **??**.

Test setup and structural response

Addressed questions:

- How to identify a bond law describing the bond behavior between matrix and reinforcement?
- How to design a test for the calibration of the bond characteristics?
- What kinds of tests exist? What are their advantages and disadvantages?
- Which tests are appropriate for the different types of reinforcement? (steel, carbon/-glass fiber-reinforced polymer, carbon or glass textile fabrics reinforcement.

1.1 Pullout test setup

First standardized pullout test

The development of a test suitable for characterization of the bond behavior between a reinforcing steel bar and concrete matrix dates back to sixties. The RILEM-FIB-CEB recommendation test has been proposed in 1973. Fig. 1.1 shows the prescribed boundary conditions and measuring equipment that records the pull-out curve in terms of the pull-out force versus slip displacement of the bar at the loaded s_l and unloaded s_u free ends. The loading process is controlled by the prescribed pullout displacement and the corresponding force is recorded. In this way, also pullout curve with diminishing force after the peak value can be measured.

The curves displayed in right diagram of Fig. 1.1 exemplify two observations that can be made using this test setup:

- The pullout curve strongly depends on the embedded length and on the diameter of the bar.
- The displacement measured at the loaded and unloaded end differ and this difference is strongly affected by the embedded length.

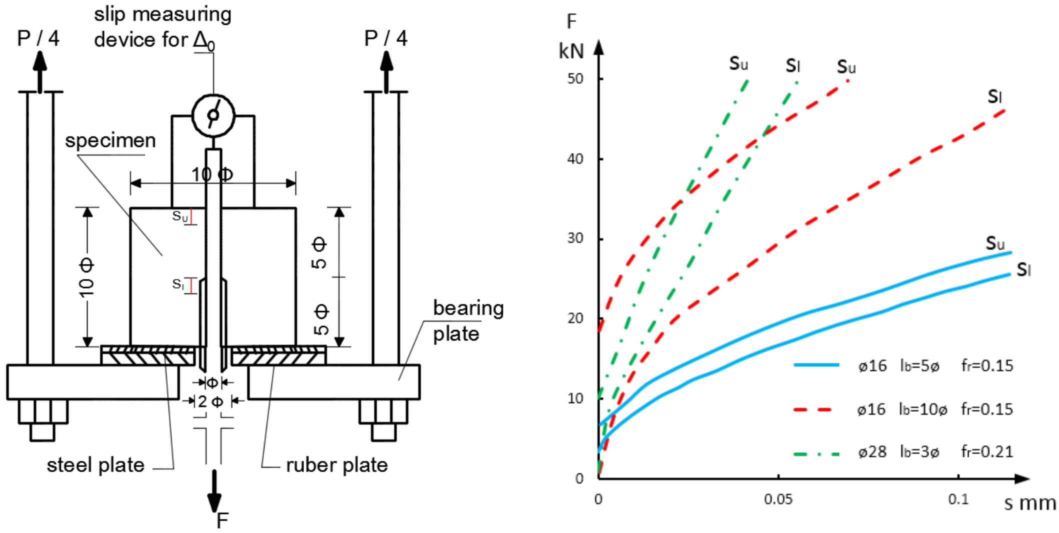

Figure 1.1 RILEM pull-out test to characterize the bond between steel and concrete.

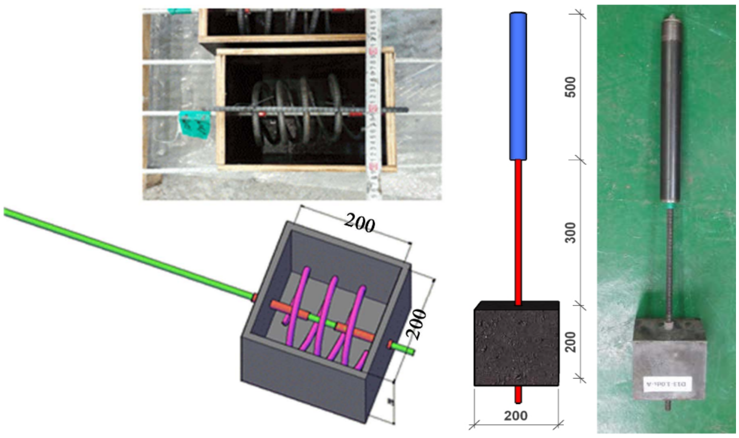

Figure 1.2 Pullout of GFRP bar from the concrete matrix.

Obviously, the experimentally observed trends must be governed by the principles of physics and mechanics. It is our ambition to capture the underlying phenomena of the bond behavior with the goal to predict the pullout behavior for changed test parameters.

Derived pull-out tests

But before approaching a more fundamental view to the effects governing the bond behavior let us span the scope of the bond description to other materials and other types of test setup. A similar type of the pullout test setup has been used to test the behavior of nonmetallic reinforcement as exemplified in Fig. 1.2. Notice that in both mentioned pullout test setups, the bond zone is located inside the specimen and there is a bond-free zone of a predefined depth starting at the loaded side. This bond-free zone is introduced with the goal to render uniform material properties along the tested bond length and to avoid the effect of a boundary zone.

Undesired compression

The described pullout test setup is very common in practice, primarily to its simplicity. However, it is not ideal in all situations because it does not really correspond to the situation in the structural elements. The reason is that due to the placement of supports at the loaded side of the specimen, non-negligible compressive stresses develop within bond zone of the concrete matrix. Such a stress state does not represent the state in the bond zone

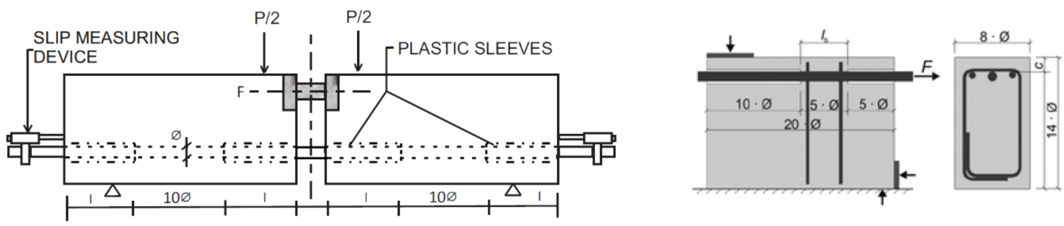

Figure 1.3 Beam tests focused on the bond characterization.

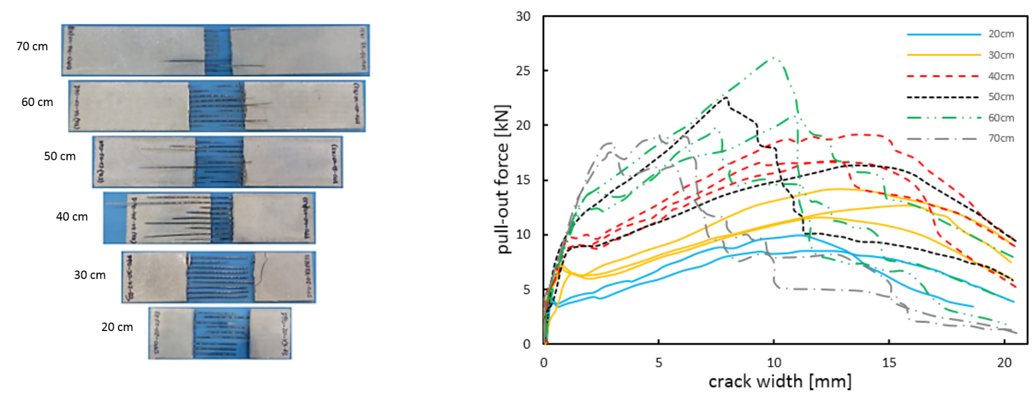

Figure 1.4 Double sided pullout test applied to carbon textile fabrics.

of a structural element which is mostly loaded in tension. As documented by experimental studies, e.g. in [**de2008bond**] the effect on the bond behavior is significant.

Beam anchorage test

The refined setup for bond characterization has been proposed in the form of beams or beam-end-sections as exemplified Fig. 1.3. Apparently, this test configuration is closer to the condition of a crack in a tensile zone of a structural specimen. The pullout displacement is measured as the opening of the crack. The test is controlled by the vertical displacement and the corresponding load is measured. It is important to note that the debonding propagates in both directions. Symmetry of the debonding process is provided until the ultimate load has been achieved. Once the pullout force has been reached at one side, the process becomes non-symmetric. As we shall discuss later on, this might become a problem in cases of materials that exhibit a so called bond softening. However, in case of steel rebars this test configuration provides a suitable solution.

Beam-end test

Further step in the development of experimental methods for the bond characterization is depicted in Fig. 1.3; right showing the beam-end test. Its boundary conditions, i.e. the placement of supports and loading are designed with the goal to render the stress state equivalent to the end zone of a tensile reinforcement in a beam. It aims to combine the positive features of both the pull-out test and of the beam anchorage test.

Test setups for fine-scale reinforcement

In case of flexible, fine scale reinforcement further types of test setups for bond characterization have been developed. An example of such a test is shown for testing the pullout behavior of textile fabrics. An example in Fig. 1.4 shows a test series performed on double sided pullout test of textile fabrics. The planar test specimens were clamped using steel plates positioned near to the middle section containing a notch and pulled apart. The opening of the notch that we refer to as crack opening displacement (COD) was recorded

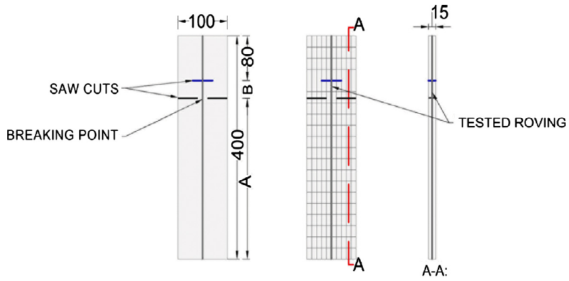

Figure 1.5 Double sided pullout test for a single fiber with a predefined pullout length at one side using a cut at one side.

during the test. This test setup can be seen in analogy to the beam anchorage length rendering a symmetric debonding on both sides up to the maximum pullout force. From there on, the process becomes non-symmetric. This fact makes it impossible to characterize the bond in material exhibiting a so called softening, i.e. decreasing shear for increasing slip after the peak value. Up to the peak, the end slip can be assumed as a half of the crack-opening displacement $s = COD/2$.

To cover also the bond behavior exhibiting softening, a small-scale test setup depicted in Fig. 1.5 has been proposed. This test setup has been derived from the double sided test setup with the goal to prescribe which side will start debonding. This test setup demonstrates the dilemma involved in the pullout test design. The stress profile should be as close as possible to the condition of crack bridge. Let us remark, that the test response must be treated with care as it contains the transition from a symmetrical debonding to a non-symmetrical one.

The brief survey of test setups demonstrates the existing variety of characterization methods that are specialized for individual types of materials. The purpose of this survey is to motivate a unified view to these experimental setups using the objective description of the bond behavior that is independent on the particular test configuration. The theoretical description of the correspondence between the local bond behavior and the global (structural) response of the pullout test is a must for a sound and detailed interpretation of experimental data.

Question: The double sided pullout test includes two debonded zones. Can we simply say that the whole process is symmetric and just calculate the pullout displacement at one side by setting $w = COD/2$?

1.2 Objectivity of a material model

The bond-slip law represents an objective material property characterizing the material behavior at any point within the interface. Fig. 1.6 shows the bond-slip law $\tau(s)$ defining the material behavior at any material point x along the embedded length.

The structural behavior that is measurable as a force-displacement relationship is represented by the pull-out curve $P(w)$ relating the displacement of the loaded fiber or reinforcement end with the applied pull-out force. Given a continuous slip $s(x)$ along the interface we can visualize the pullout force P as the green area representing the integral

$$P = \int_0^L \tau(s(x))\,\mathrm{d}x.$$

By identifying a "true" bond-slip law we get the possibility to predict the pull-out curve for diversity of loading scenarios. It is the key to the prediction of structural response. The question is how to identify the bond slip law from an experimental observation, e.g. from the measured pull-out curve $P(w)$.

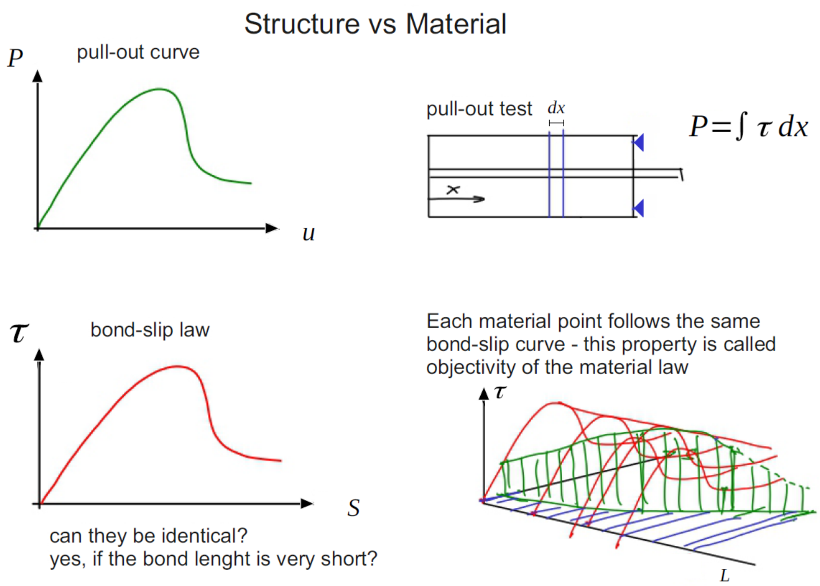

Figure 1.6 Relation between material behavior and structural behavior

A simple experimental strategy to identify the bond slip law attempts to use a very short embedded length with the goal to achieve a uniform slip along the whole interface length. Then, the front and end slip of the pullout test are the same. In such a case, the pull-out curve can be directly transformed to the bond-slip relation by dividing the force with the interface area given as the product of the perimeter p and length L

$$\tau(s) = \frac{1}{pL} P(s).$$

However, it is rather difficult to design such a short test setup in a reproducible way. The short section of the material along the interface zone exhibits a relatively large scatter of properties so that many tests have to be conducted. Furthermore, the production of small size specimens results in a material behavior that is different from the *in-situ* conditions.

Realistic prediction of the pullout behavior is needed to support both the efficient and goal oriented material design with tuned material behavior. At the same time, it provides a valuable input for the formulation of design codes. In the sequel we will exemplify this issue on the example of the identification of the anchorage length.

The structural configuration of the pullout test is depicted in Fig. 1.7, including the elastic parameters of the material components. The Figure also shows the boundary conditions BC1, BC2 that can be considered to solve the pullout test. The boundary condition BC3 with the clamped reinforcement represents a configuration of a crack bridge in a tensile test that we will discuss in the context of a multiple cracking behavior of brittle-matrix composites.

*S*1

[*S1*:] can I add Parameters'(Lb, Lf, A, E, etc.) definition on the right side of the figure?

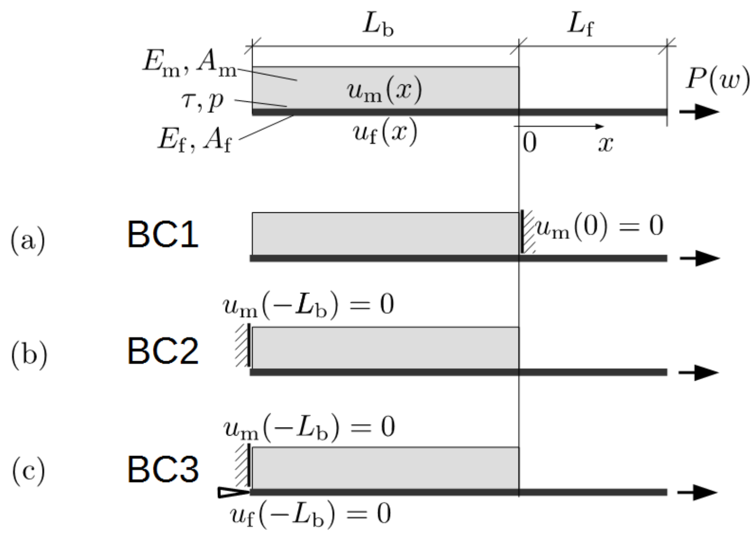

Figure 1.7 One dimensional idealization of the pullout test as boundary value problem

All the displayed configurations can be associated with different types of material behavior. If we assume rigid matrix and constant or linear bond-slip law, it is possible to derive analytical solutions of the pullout problem.

In case of a generally non-linear bond slip law, including inelastic effects, like friction and damage, numerical solutions are available. In Sec. 1.3 we will construct a simple analytical solution of the pullout problem that can cover all the configurations depicted in Fig. 1.7. Each model will be accompanied with an executable script providing the possibility to study the effect of the geometrical and material parameters on the response of the pullout test.

1.3 Analytically solvable pullout problems

Special case of bond behavior used for quick characterization of bond is described by a constant bond-slip function.

$$\tau(s) = \bar{\tau} \tag{1.1}$$

With this assumption, we can derive an analytic expression for the relation between the pull-out force P versus pull-out displacement $u_{\mathrm{f},0}$. This solution deserves our attention because of its frequent use in interpretation of experimental results of pull-out tests and also in design rules for composite materials. Therefore, it is helpful to understand the correspondence between the stress, strain and displacement profiles and the boundary conditions.

The most simple theoretical description of a non-linear structural behavior is provided for the uni-axial idealization of the pullout test assuming a frictional type of bond exhibiting a stick-slip behavior. The assumed shape of bond law is sketched in Fig. 1.8.

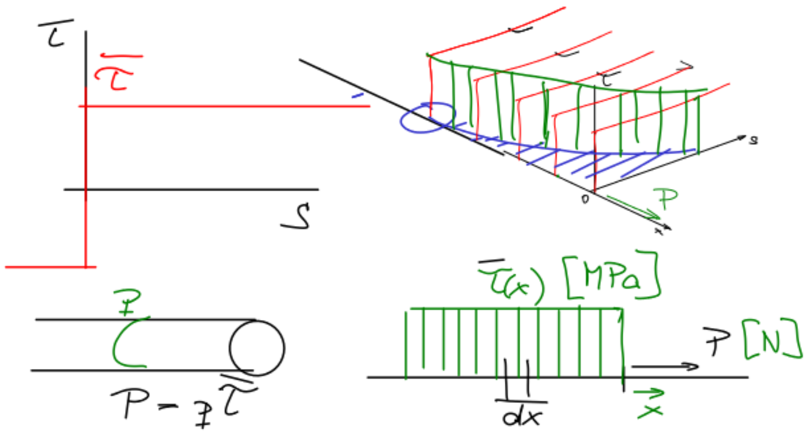

Figure 1.8 Assumptions included in the pullout-model with constant bond stress

1.3.1 Constant shear bond to a rigid matrix

Regarding an infinitesimal element of an interface area within a composite cross section shown in Fig. 1.9 we can formulate the local equilibrium condition as

Just one unknown field $u_\mathrm{f}(x)$

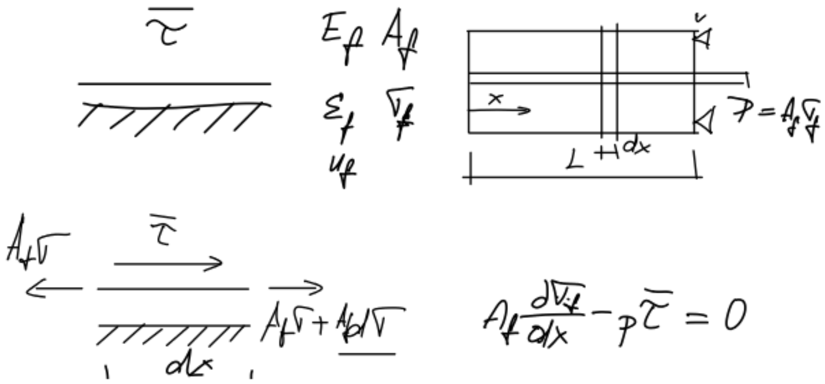

Figure 1.9 Variables and parameters describing the constant bond model

$$A_\mathrm{f}\, \sigma_{\mathrm{f},x} - p\bar{\tau} = 0 \tag{1.2}$$

where A_f is the area of the reinforcement, $\sigma_{\mathrm{f},x}$ the derivative of the fiber stress with respect to the the length coordinate x, p is the perimeter, and $\bar{\tau}$ stands for the constant shear/frictional bond stress. Integration of Eq. (1.2) reveals that the stress $\sigma(x)$ is linear, i.e.

Local equilibrium

$$\sigma_\mathrm{f}(x) = \frac{p\bar{\tau}}{A_\mathrm{f}} x + C \tag{1.3}$$

Assuming a linear elastic reinforcement behavior with the material stiffness E_f at every point x of the reinforcement ($\sigma_\mathrm{f} = E_\mathrm{f}\varepsilon_\mathrm{f}$) we rewrite this condition for strain along the debonded zone as

$$\varepsilon_\mathrm{f}(x) = \frac{1}{E_\mathrm{f}}\sigma_\mathrm{f}(x) = \frac{1}{E_\mathrm{f}}\left(\frac{p\bar{\tau}}{A_\mathrm{f}} x + C\right) \tag{1.4}$$

Kinematics

and then into the kinematic condition

$$u_\mathrm{f} = \int \varepsilon_\mathrm{f}(x)\,\mathrm{d}x = \frac{1}{E_\mathrm{f}}\left(\frac{p\bar{\tau}}{2A_\mathrm{f}}x^2 + Cx\right) + D = \frac{1}{2}\frac{p\bar{\tau}}{E_\mathrm{f}A_\mathrm{f}}x^2 + \frac{1}{E_\mathrm{f}}Cx + D \tag{1.5}$$

we obtain the quadratic function of the reinforcement displacement with the two parameters C, D to be determined using the boundary conditions.

Resolve constants

To determine the constant C we recall that the force distribution along the bar given as

$$F_\mathrm{f}(x) = \sigma_\mathrm{f}(x)A_\mathrm{f} = p\bar{\tau}x + CA_\mathrm{f}, \tag{1.6}$$

must be equal to the applied load P at the pulled end $(x = 0)$, i.e.

$$F(0) = \sigma_\mathrm{f}(0)A_\mathrm{f} = P \qquad \Longrightarrow \qquad C = P/A_\mathrm{f}. \tag{1.7}$$

Global equilibrium

By substituting Eq. (1.7) into Eq. (1.5) the displacement field of the reinforcement can be rewritten as

$$u_\mathrm{f}(x) = \frac{1}{2}\frac{p\bar{\tau}}{E_\mathrm{f}A_\mathrm{f}}x^2 - \frac{P}{E_\mathrm{f}A_\mathrm{f}}x + D. \tag{1.8}$$

Compatibility

To factor out the parameter D another condition is needed. This condition can be introduced by realizing that in zones, where the reinforcement is still bonded to the matrix, there is no slip and, thus, the displacement in the reinforcement at point a is zero. Knowing that the debonded zone starts from the loaded end and propagates inwards through the bond layer, we can require

$$u_\mathrm{f}(a) = 0 \qquad \Longrightarrow \qquad D = -\frac{a}{2A_\mathrm{f}E_\mathrm{f}}(2P + ap\tau) \tag{1.9}$$

Still, the problem has one unknown variable, namely the debonded length a. To resolve it, we need another condition. Realizing that also the strain at a must vanish we can substitute a for x in Eq. (1.4) and resolve for the state variable a to get

$$\varepsilon_\mathrm{f}(a) = 0 \qquad \Longrightarrow \qquad a = -\frac{P}{p\bar{\tau}}. \tag{1.10}$$

State fields

With all the variables at hand, the sought reinforcement displacement corresponding to the given boundary conditions has the form

$$u_\mathrm{f}(x) = \frac{1}{2}\frac{p\bar{\tau}}{E_\mathrm{f}A_\mathrm{f}}x^2 - \frac{P}{E_\mathrm{f}A_\mathrm{f}}x + \frac{1}{2E_\mathrm{f}A_\mathrm{f}}\frac{P^2}{p\bar{\tau}}. \tag{1.11}$$

Particularly interesting is the displacement at the loaded end $u(x = 0)$

$$u_\mathrm{f}(0) = w = \frac{1}{2}\frac{P^2}{p\bar{\tau}E_\mathrm{f}A_\mathrm{f}}. \tag{1.12}$$

Pullout curve

By solving this equation for P we finally obtain an explicit function describing the pull-out curve in the form

$$P(w) = \sqrt{2p\bar{\tau}E_\mathrm{f}A_\mathrm{f}w}. \tag{1.13}$$

Example 1.1: Pullout from rigid matrix

Question: Consider the pullout test depicted in Fig. 1.1. Evaluate the pullout curve assuming that there is deformation in concrete and that the bond behavior corresponds to the purely frictional bond derived previously. The boundary value problem idealizing such structural behavior is depicted in Fig. 1.7ab.

Solution: A python script evaluating the problem using the derived model (1.13) has been prepared here to perform calculations using the model. It can be readily used to test the model and evaluate the pullout curves and also the stress, strain and displacement fields. Exemplified results are provided here for the values of parameters

$$E_{\mathrm{f}} = 1, \quad A_{\mathrm{f}} = 1, \quad \bar{\tau} = 1, \quad L_{\mathrm{b}} = 1 \tag{1.14}$$

Results: The top-left diagram shows the $P(w)$ curve, the top right diagram shows the slip along the bond length for several load levels, the bottom diagrams visualize the strain and stress along the bond length. Since $E_{\mathrm{f}} A_{\mathrm{f}} = 1$, they are equal.

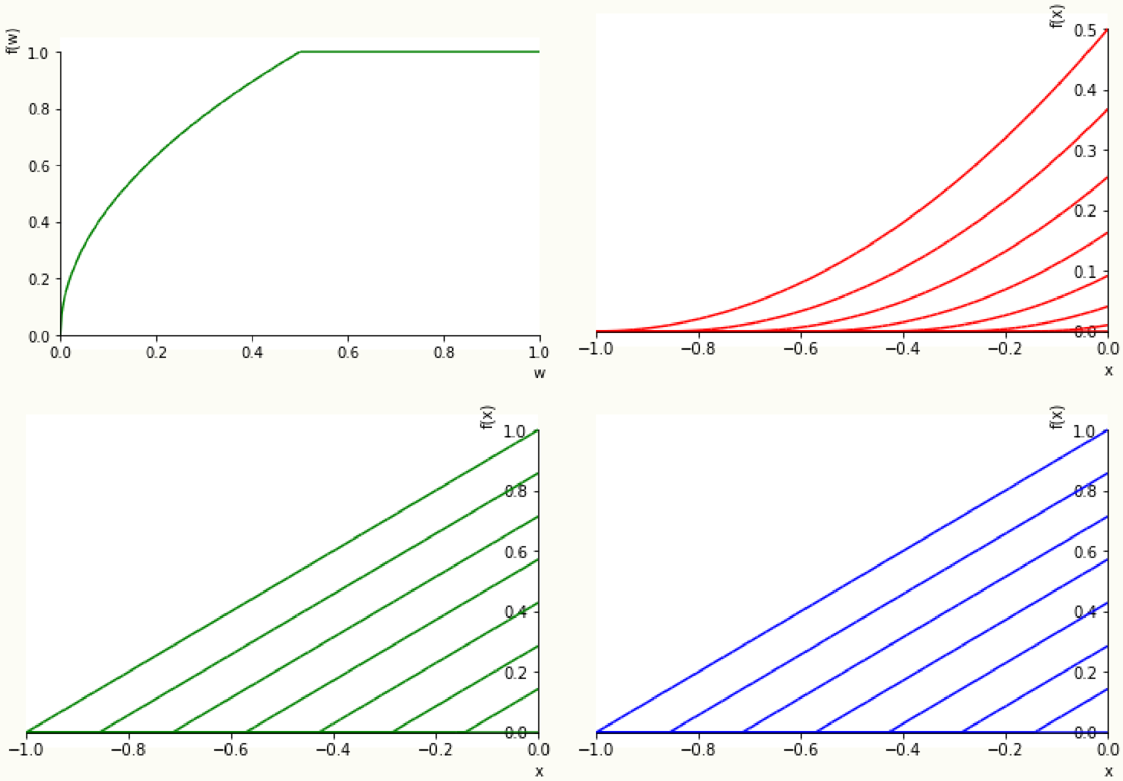

Task: Change the material parameters given in the script to reproduce the test results of the RILEM pullout test presented in Fig. 1.1. Is it possible to set up the model such that it can reproduce the results?

Example 1.2: Pullout from rigid matrix with extra bar length at the loaded end

Question: The bar in test shown in Fig. 1.1 does not start immediately at the beginning of the bonding zone. Extend the model by including the deformation of the bar along the free length such that it is possible to place the LVDT measuring the displacement on the steel bar at some distance from the bond zone. In the evaluation use the parameters

$$E_\mathrm{f} = 1, \quad A_\mathrm{f} = 1, \quad \bar{\tau} = 1, \quad L_\mathrm{b} = 1, \quad L_\mathrm{f} = 1 \tag{1.15}$$

Solution: The required extension of the analytical model requires another spring attached to the model previously derived and to impose a compatibility codition. The derivation has been done using the symbolic algebra package in the Python language. The executable jupyter notebook can be downloaded here.

Results: The diagrams demonstrate the difference with respect to Example 1.1 for $P(w)$ pullout curve, displacement, strain and stress fields along the bar.

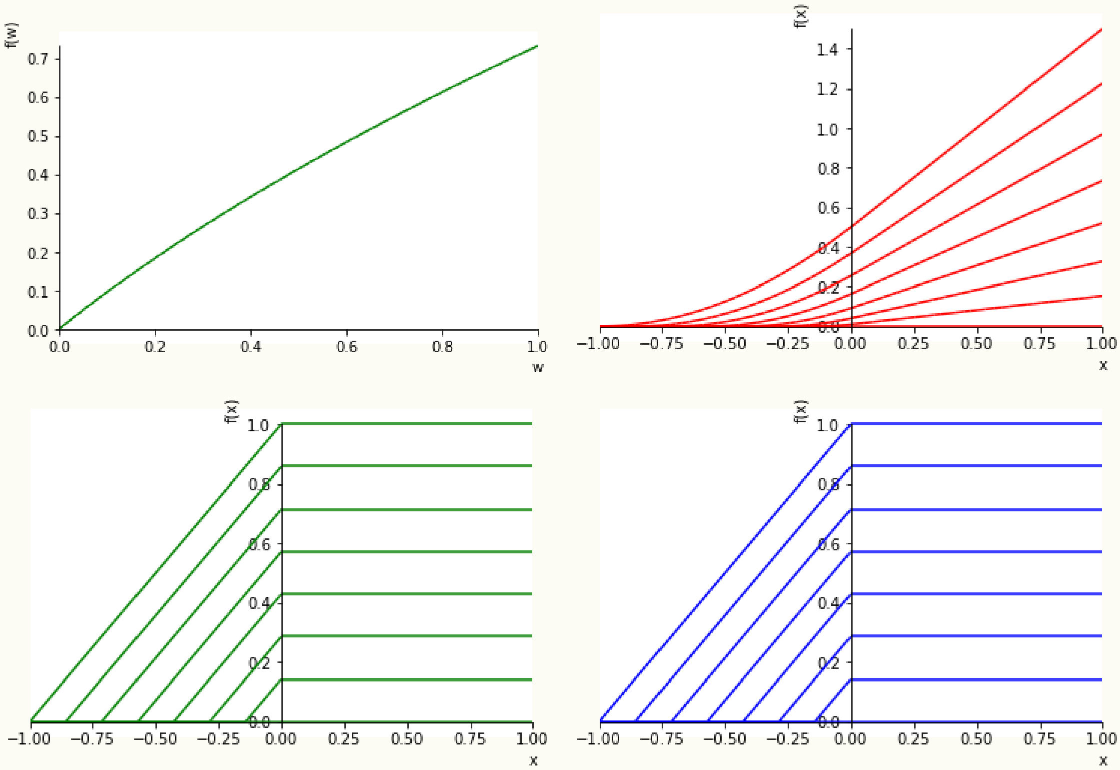

Task: Test the effect of the changing free bar length. How does the pullout curve $P(w)$ look like qualitatively if the free length of the bar gets very long?

Task: Name all possibilities how this pullout test can ultimately fail.

1.3.2 Constant shear bond to elastic matrix

What if the matrix deforms as well?

An extension of the previous model for elastic matrix can be done by refining the condition of compatibility. Let us exemplify this extension for two kinds of boundary conditions depicted in Fig. 1.10. Given the strain in the concrete matrix and in the fabric reinforcement, ε_m and ε_f, respectively we can evaluate the relative slip at $x = 0$ as

$$w = \int_{-a}^{0} \varepsilon_\mathrm{f} - \varepsilon_\mathrm{m} \, \mathrm{d}x. \tag{1.16}$$

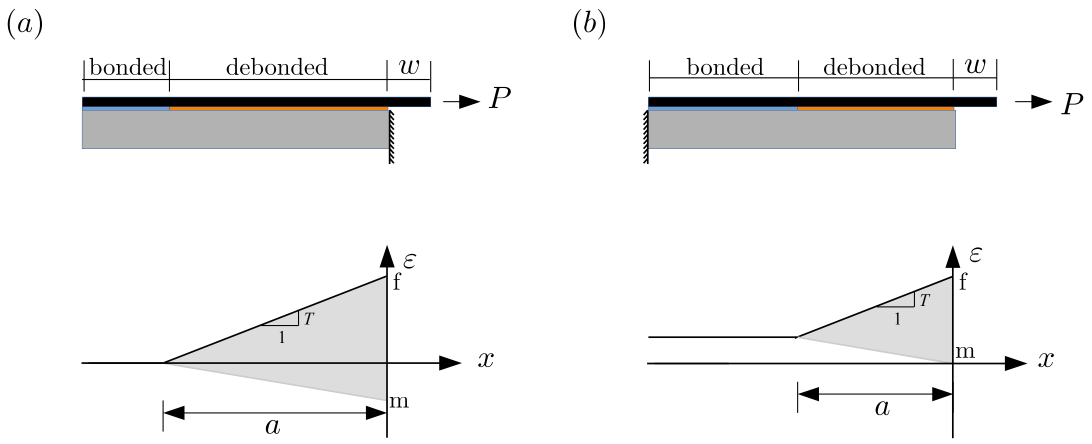

Figure 1.10 Profile of strains in the pullout-model with constant bond stress; a) Matrix supported at loaded end, b) Matrix supported at unloaded end

It is represented by the shaded area in Fig. 1.10. In the simple case of constant bond, the area is of triangular shape so that the derivation can be simplified. In order to determine the area of the triangle, the following parameters are required: the strains $\varepsilon_\mathrm{f}(x=0)$ and $\varepsilon_\mathrm{m}(x=0)$, as well as the debonded length a.

1.3.2.1 Matrix supported at the loaded end (BC1)

When the matrix is fixed at $x=0$ as shown in Fig.1.10a, the required parameters can be determined as

$$\varepsilon_\mathrm{f}(0) = \frac{P}{E_\mathrm{f}A_\mathrm{f}}, \quad \varepsilon_\mathrm{m}(0) = \frac{-P}{E_\mathrm{m}A_\mathrm{m}} \tag{1.17}$$

$$T = \frac{p\tau}{E_\mathrm{f}A_\mathrm{f}} \tag{1.18}$$

$$a = \frac{\varepsilon_\mathrm{f}(0)}{T} = \frac{P}{p\tau}. \tag{1.19}$$

Thus, the crack opening can be expressed as the area of the triangle

$$\begin{aligned} w &= \frac{1}{2}\left[\varepsilon_\mathrm{f}(0) - \varepsilon_\mathrm{m}(0)\right] a \\ &= \frac{1}{2}\frac{P^2}{p\tau}\left[\frac{1}{E_\mathrm{f}A_\mathrm{f}} + \frac{1}{E_\mathrm{m}A_\mathrm{m}}\right]. \end{aligned} \tag{1.20}$$

By solving this equation for P we obtain the pullout curve in the form

$$P(w) = \sqrt{2wp\tau\frac{E_\mathrm{f}A_\mathrm{f}E_\mathrm{m}A_\mathrm{m}}{E_\mathrm{f}A_\mathrm{f} + E_\mathrm{m}A_\mathrm{m}}}. \tag{1.21}$$

Example 1.3: Pullout from elastic matrix clamped right

Pullout from rigid matrix with extra bar length at the loaded The described procedure can be applied with further extensions considering different position of supports, inclusion of free-length of the reinforcement at the pulled-out end. The script containing this model is provided here.

Task: Use the model with the material parameters appropriate to carbon reinforcement and concrete with the stiffness $E_\mathrm{m} = 28$ GPa and find out for which ratio of cross-sectional areas $A_\mathrm{m}/A_\mathrm{m}$ does the pull-out curve change.

1.3.2.2 Matrix supported at unloaded end (BC2)

For the case shown in Fig.1.10b where the matrix is fixed at the left side, the values of $\varepsilon_\mathrm{f}(x = 0)$ and T remain the same, while

$$\varepsilon_\mathrm{m}(x = 0) = 0 \tag{1.22}$$

$$\varepsilon_\mathrm{f}(x = -a) = \frac{P}{E_\mathrm{f}(A_\mathrm{m} + A_\mathrm{f})}, \tag{1.23}$$

and the debonded length

$$a = \frac{\varepsilon_\mathrm{f}(x = 0) - \varepsilon_\mathrm{f}(x = -a)}{T} \tag{1.24}$$

$$= \frac{P A_\mathrm{m}}{p\tau(A_\mathrm{f} + A_\mathrm{m})}. \tag{1.25}$$

Then the slip at $x = 0$ can be written as

$$w = \frac{1}{2}\frac{P^2 A_\mathrm{m}}{p\tau E_\mathrm{f} A_\mathrm{f}(A_\mathrm{f} + A_\mathrm{m})} \tag{1.26}$$

and finally the pull-out response is given by

$$P(w) = \sqrt{2wp\tau\frac{E_\mathrm{f} A_\mathrm{f}(A_\mathrm{f} + A_\mathrm{m})}{A_\mathrm{m}}} \tag{1.27}$$

Example 1.4: Pullout from elastic matrix clamped left

Pullout from rigid matrix with extra bar length at the loaded The described procedure can be applied with further extensions considering different position of supports, inclusion of free-length of the reinforcement at the pulled-out end. The script containing this model is provided here.

Task: Use the model with the material parameters appropriate to carbon reinforcement and concrete with the stiffness $E_\mathrm{f} = 28\ GPa$ and find out for which ratio of cross-sectional areas $A_\mathrm{m}/A_\mathrm{m}$ does the pull-out curve change.

Task: Answer the question: Assuming steel rebar, at which level of reinforcement ratio does the elasticity of matrix change the maximum pullout force by 10% compared to the case of rigid matrix?

1.3.3 Piecewise linear bond-slip law

Besides the case of the frictional model, analytical solution can be derived also for linear-elastic bond as presented in [**one**] S2 [S2:] Can I correct the citation number? one?

$$P(u_{\mathrm{f},0}) = \frac{k\tanh(\alpha L)}{\alpha} u_{\mathrm{f},0}, \quad \text{with } \alpha = \sqrt{pk\left(\frac{1}{E_\mathrm{f} A_\mathrm{f}} + \frac{1}{E_\mathrm{m} A_\mathrm{m}}\right)} \tag{1.28}$$

This solution can describe the initial stages up to the onset of debonding. Notice that the relation the function $P(w)$ is linear. This solution can be generalized for piecewise linear bond-slip law as exemplified in [**yuan_full-range_2004**]. Then a solution of the pullout problem with non-linear bond-slip law can obtained by putting together the analytical solutions along every segment. However, a more general and efficient solution can be obtained within the framework of the standard non-linear finite element solver. In the following chapter such a solver will be presented including the executable code to solve examples.

1.4 Conclusions and remarks

This class of pull-out models is particularly useful as a basic component of models studying statistical aspects of scatter in heterogeneous materials in the vicinity of crack bridges.